

Terahertz Gunn-like oscillations in InGaAs/InAlAs planar diodes

S. Pérez,^{a)} T. González, D. Pardo, and J. Mateos

*Departamento de Física Aplicada, Facultad de Ciencias, Universidad de Salamanca, Plaza de la Merced
whis/n, 37008 Salamanca, Spain*

(Received 8 January 2008; accepted 2 March 2008; published online 9 May 2008)

A microscopic analysis of self-generated terahertz current oscillations that take place in planar InAlAs/InGaAs slot diodes operating under dc bias is presented. An ensemble Monte Carlo simulation is used for the calculations. The onset of the oscillations is thresholdlike, for drain-source voltages surpassing 0.6 V. The Gunn-like mechanisms and the modulation of the injection of electrons into the recess-to-drain region, which alternatively takes place in the Γ or L valley, are found at the origin of the phenomenon. Terahertz frequencies are reached because of the presence of ultrafast Γ electrons in the region of interest. Extremely high velocities are achieved by (i) the effect of the recess, which focuses the electric field and launches very fast electrons into the drain region, and (ii) the influence of degeneracy, which significantly reduces the rate of scattering mechanisms and enhances the electron mobility in the channel. © 2008 American Institute of Physics. [DOI: 10.1063/1.2917246]

I. INTRODUCTION

Terahertz radiation (100 GHz–10 THz), which is also known as a T -ray, provides a huge potential in the fields of imaging, ranging, spectroscopy, and guidance, which could be of strong interest for a number of medical, robotics, security, and military applications.¹ The terahertz frequency range lies between microwaves and infrared light in the electromagnetic spectrum; thus, the technology for producing T -ray sources is at the limits of electronics from one side and optical systems from the other. Indeed, no powerful radiation sources have been available until the past few years.^{2,3} Even with the strong advances obtained with quantum cascade lasers (at cryogenic temperatures). Nowadays, it does not exist yet a compact, room temperature, high-power source that is well controlled, tunable, and suitable for the terahertz frequency range. From the practical point of view, the most interesting solution seems to be the terahertz sources based on solid state devices, which offer the best possibilities of integration with other electronic or optoelectronic devices within a single chip.¹

Recent measurements in nanometer gate length InAlAs/InGaAs high electron mobility transistors (HEMTs) have shown the emission of radiation at terahertz frequencies.^{4,5} Initially, the mechanism for terahertz emission in HEMTs was identified as the result of plasma wave generation due to the Dyakonov–Shur instability.⁶ However, the thresholdlike behavior of the terahertz emission (when increasing the drain bias) and the associated kinks that appear in the I - V curves indicate that, instead of plasma instabilities, a hot carrier mechanism such as the Gunn effect could be responsible for the high-frequency oscillations.^{7,8}

In this work, we present a detailed Monte Carlo (MC) study of current oscillations in the ungated heterostructures on which these HEMTs are based. For this sake, we perform calculations of the current noise spectra, which can give pre-

cise indications on the onset of collective phenomena such as plasma or Gunn oscillations. Although this oscillatory behavior has also been found in nanometer gate length InAlAs/InGaAs HEMTs, ungated HEMT-like heterostructures (also called slot diodes) are chosen for simplicity because the gate terminal is not essential to start the oscillations. The fundamental point is the localization of a strong potential drop across a narrow region, which is an effect obtained by means of a recess. We will show that the ultrafast Gunn-like phenomena that take place in these planar diodes lead to current oscillations in the terahertz range. Gunn oscillations due to the transfer of electrons to the upper valleys in the gate-drain region of HEMTs or in planar AlGaAs/GaAs heterostructures have already been experimentally observed and found in MC simulations;^{9,10} however, they usually exhibit much lower frequencies. In order to reach oscillation frequencies in the terahertz range, the high-field domain must travel much faster than the saturation velocity of the electrons in the channel. This paper proposes the geometry and explains the physics of a novel form of a planar ultrafast Gunn-like diode that is capable of producing these extremely high-frequency oscillations. Remarkably, the topology of this planar two terminal device makes it ideally suited for integration into monolithic microwave integrated circuits (MMICs) in contrast to conventional Gunn diodes. This fact facilitates the developing of the terahertz technology toward portable and much less costly systems.

The paper is organized as follows: In Sec. II, the physical system under analysis together with the details of the MC simulation are described. In Sec. III, the results obtained for the static characteristics and the oscillatory behavior of the diodes are reported. Section IV summarizes the main conclusions and future lines of our work.

II. PHYSICAL MODEL AND MONTE CARLO SIMULATION

The layer structure of the simulated slot diodes is shown in Fig. 1. It consists of a 200 nm In_{0.52}Al_{0.48}As buffer fol-

^{a)}Electronic mail: susana@usal.es.

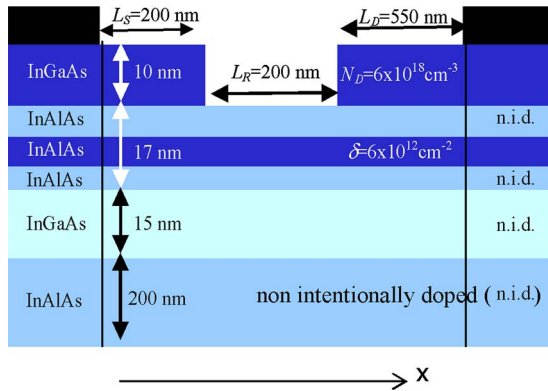


FIG. 1. (Color online) Geometry of the simulated InAlAs/InGaAs slot diode (note that the X axis is used in Figs. 4–6).

lowed by a 15 nm thick $\text{In}_{0.70}\text{Ga}_{0.30}\text{As}$ channel, three layers of $\text{In}_{0.52}\text{Al}_{0.48}\text{As}$ (a 3 nm spacer, a $6 \times 10^{12} \text{ cm}^{-2}$ δ doping modeled as a 4 nm layer doped at $N_D = 1.5 \times 10^{19} \text{ cm}^{-3}$, and a 10 nm Schottky layer) and, finally, a 10 nm thick $\text{In}_{0.53}\text{Ga}_{0.47}\text{As}$ cap ($N_D = 6 \times 10^{18} \text{ cm}^{-3}$). Note that this layer structure is the base for the realization of real InP based HEMTs.^{7,8,10} A key parameter in the geometry of the diode is the recess-to-drain distance, which is 550 nm in the simulated diode.

Calculations are performed by using an ensemble MC simulator at room temperature, which is self-consistently coupled with a two dimensional Poisson solver. The material parameters and microscopic models are reported in Ref. 11. The devices are divided into 5 nm long and 1–10 nm wide meshes depending on the doping and the required resolution of the potential along the structure. The Ohmic boundary conditions are considered in the source and drain contacts, which are vertically placed adjacent to different materials.¹¹ Accordingly, nonuniform potential and concentration profiles are considered along these contacts, those that would be obtained if real top electrodes were simulated.¹¹

The effect of degeneracy is accounted for by locally us-

ing the classical rejection technique, where the electron heating and nonequilibrium screening effects are introduced by means of the local electron temperature. No other quantum effects are considered in the simulation in order to have reasonable CPU times. The validity of this approximation (especially under high-field conditions) and that of the whole MC model was confirmed in previous works.^{11,12}

In order to detect and emphasize the presence of plasma or Gunn oscillations, special attention is devoted to the calculation of noise spectra due to their extreme sensitivity to microscopic features of carrier dynamics and the possibility to easily perform a frequency analysis of the electrical fluctuations.

III. RESULTS

The static current-voltage characteristic of the slot diode is shown in Fig. 2. It can be observed that a kink appears just when the Γ - L intervalley transfer starts to be important in the InGaAs channel, for V_{DS} about $V_{th} = 0.6 \text{ V}$ (the Γ - L energy separation is 0.61 eV). For voltages above V_{th} , current oscillations (caused, as we will see, by an ultrafast Gunn-like effect) clearly appeared (right inset). These are coherent oscillations that give birth to a pronounced peak in the current spectrum [as shown in Fig. 2(b)] and also to a decrease mean value of the current [producing the kink observed in the I - V curves, Fig. 1(a)]. Plasma oscillations that appear for low applied voltages are noncoherent and also provide a peak in the current noise spectrum, as shown in Fig. 2(c). However, this peak is easily distinguished from that provided by Gunn-like oscillations, first because it lies at much higher frequencies, and second, because its amplitude is much lower. These differences are observed in Fig. 3 where the frequency and amplitude of the main peak that is found in the current noise spectrum are plotted as a function of the applied bias. The high-amplitude Gunn-like oscillations, with a frequency around 1 THz, appear for $V_{DS} > V_{th}$, while for lower voltages, there are only low-amplitude higher-frequency plasma oscil-

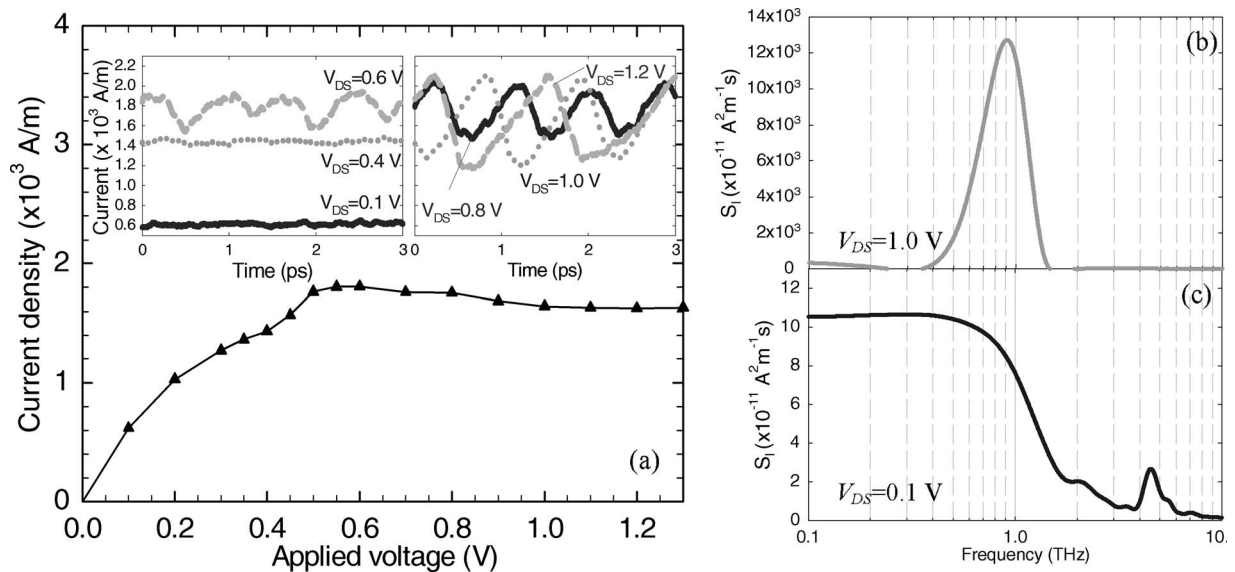


FIG. 2. (a) Static I - V characteristic of the slot diode. The insets show the time-varying current for different applied voltages: $V_{DS} \leq 0.6 \text{ V}$ (left inset) and $V_{DS} > 0.6 \text{ V}$ (right inset). [(b) and (c)] Spectral density of current fluctuations for $V_{DS} = 1.0 \text{ V}$ and $V_{DS} = 0.1 \text{ V}$, respectively.

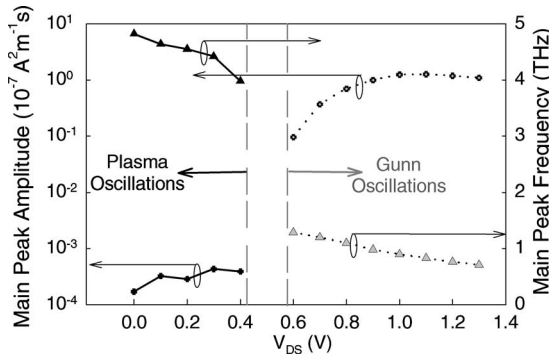


FIG. 3. Amplitude (crosses, left axes) and frequency (triangles, right axes) of the main peak in the spectral density of current fluctuations as a function of V_{DS} . The dotted lines indicate the V_{DS} regime where the Gunn oscillations take place.

lations (around 4.5 THz). The amplitude of these ultrafast Gunn oscillations increases, saturates, and even decreases for the highest voltages (gray circles, left axis) while the frequency (entering the terahertz range) decreases with increasing bias (gray triangles, right axis). A frequency shift of 0.78 THz is obtained by increasing the bias from 0.6 to 1.3 V. This wide frequency tunability can be very important for practical applications.

Figure 4 shows the profiles of electric field in the channel of the heterostructure at different time moments within one period of the oscillation, for $V_{DS}=1.0$ V. The presence of a peak in the electric field distribution that displaces along the recess-drain region at extremely high velocity is observed ($v_E \sim 10 \times 10^7$ cm/s). This increase in the electric field is spatially linked to a low carrier concentration in the channel, as can be observed in Fig. 5(a). Moreover, as observed in Fig. 5(b), which shows the total carrier density (and the Γ and L contributions) at $t=0$, the region with a low concentration is started by the reduced presence of Γ elec-

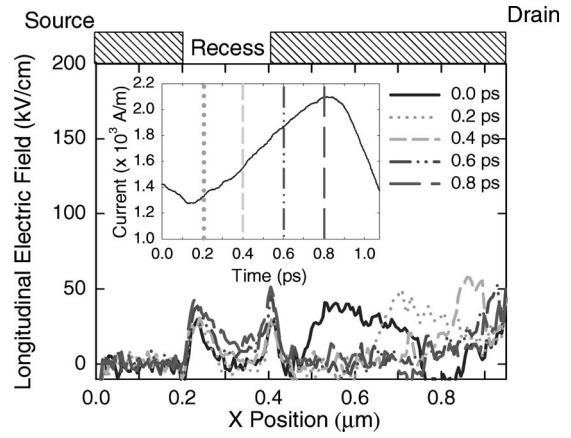


FIG. 4. Profile of the longitudinal electric field in the channel of the heterostructure at different time moments within one period of the oscillation for a bias $V_{DS}=1.0$ V. The insets show the time-varying current during one period of the oscillation.

trons, with most of the carriers populating the L valley (in a concentration similar to that of the rest of the recess-drain region).

Therefore, the oscillatory behavior of the current must be somehow related to the intervalley mechanisms that push the carriers into the upper satellite valleys. This fact is analogous to what happens in the typical Gunn diode oscillations. However, the creation and annihilation of space-charge domains in the heterostructure slot diodes exhibit important differences with respect to the behavior of classical Gunn devices. The active region for the formation and displacement of the field inhomogeneity is not the total cathode-to-anode distance but only the recess-to-drain region. Indeed, the peak in the electric field at the drain edge of the recess is responsible for the maintenance of oscillations due to the modulation of its height along a period and also for the high speed of the Γ valley electrons injected into the drain region.

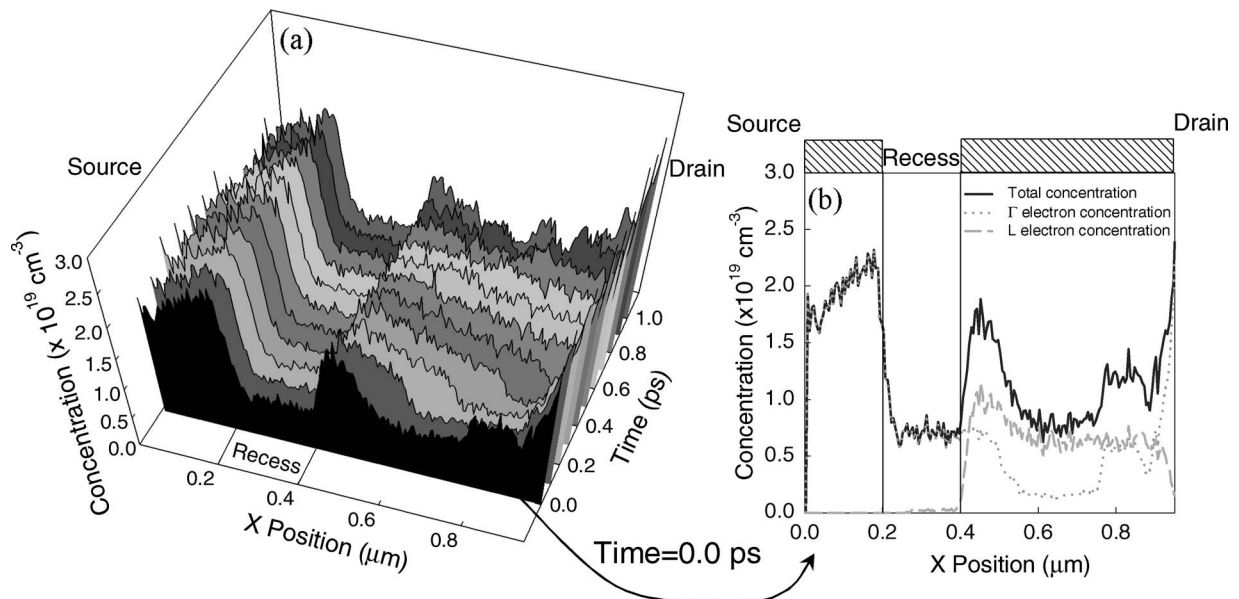


FIG. 5. (a) Profile of the carrier concentration in the channel of the heterostructure at different time moments within one period of the oscillation for a bias $V_{DS}=1.0$ V. (b) Profile of the Γ valley (dotted line), L valley (dashed line), and total carrier concentration (solid line) in the channel at a time of 0.0 ps.

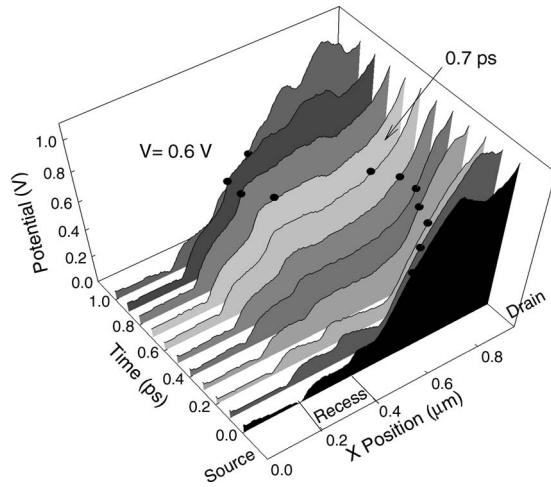


FIG. 6. Profile of the potential in the channel of the heterostructure at different time moments within one period of the oscillation for a bias $V_{DS} = 1.0$ V. The point corresponding to $V_{th} = 0.6$ V is marked in the different curves.

However, if this peak is sufficiently high (what happens at some moments during one period), it makes electrons gain enough energy to reach the L valley and almost no fast electron subsists at that point.

To understand the origin of the oscillation, it is interesting to observe the profile of the electric potential in the channel at different times within one period, as shown in Fig. 6, for an applied voltage of 1.0 V. The point at which a value of 0.6 V (energy distance between Γ and L valleys) is reached is marked by a circle in each curve. Depending on the position at which such a value is reached, electrons are injected into the recess-drain region just in the Γ valley (V_{th} reached after the recess) or both in the Γ and the L valleys (V_{th} reached at the edge of the recess). Note that due to the low effective mass of electrons in InGaAs and the high carrier concentration in the channel, Γ electrons quasiballistically move along the high-field region under the recess, without dissipating the energy gained from the electric field (very few scattering mechanisms are observed in the simulations).

In the range of 0.7–1.0 ps, the carrier concentration is essentially uniform in the recess-drain region (no depleted zone, carriers nearly equally distributed in the Γ and L valleys). The most resistive part of the device is the (low-concentration) region under the recess, where a drop of voltage higher than V_{th} takes place. As a consequence, an increasing amount of electrons jumps to the L valley near the drain edge of the recess. These electrons are very slow (compared to those in the Γ valley) and need a long time to reach the drain terminal. In contrast, Γ carriers that are injected into the drain region prior to the L electrons move very fast toward the contact, leading to a decrease in concentration near the recess, which is not compensated by new fast electrons that are injected in the Γ valley (since only L valley electrons are being injected). This produces a partially depleted region where, practically, only carriers in the L valley are present [see Fig. 5(b)]. This region of low concentration, which is initially very narrow, increases with time and absorbs a higher potential drop (see curves corresponding to 1.0, 0.0, and 0.1 ps in Figs. 5 and 6) so that the point at

which the potential reaches V_{th} moves rather inside the recess-drain region well after some time. When this happens, carriers that are injected in the recess will be mostly very fast carriers in the Γ valley that, having been accelerated by the high field in the recess region, have not reached the L valley because of the lower potential drop. These fast Γ carriers progressively fill (0.2–0.6 ps) the depleted region that was previously described until the uniform carrier concentration of the starting conditions at 0.7 ps is achieved.

The peak in the electric field that is observed in Fig. 4 takes place at the low-concentration region and moves toward the drain at the very high velocity of the Γ valley electrons filling the depleted region (10×10^7 cm/s). This is the reason for the ultrafast motion of the high-field region (Fig. 4) and the associated current oscillations. While L electrons are being injected into the recess-drain region and the depleted region increases, the current decreases, then grows when only Γ electrons are injected from the recess.

Once the threshold of 0.6 V is surpassed, as the applied voltage increases, the formation of the depleted region requires more time since it takes a longer time to move the V_{th} value of the potential far from the recess-drain edge to improve the Γ -valley injection. For the same reason, the depleted region is more pronounced. This explains the lower frequency and higher amplitude of the oscillations observed in Fig. 3 as the applied voltage increases.

It is important to remark that this ultrahigh-frequency nonstationary phenomenon is rather different from the classical Gunn effect, which is based in the propagation of a dipolar domain that always travels at the electron saturation velocity, which is slightly higher than 1×10^7 cm/s in InGaAs and, therefore, a much slower process. The ultrafast quasiballistic Γ electrons at the origin of the oscillations found in the planar heterostructures appear as a consequence of (i) the high electric field in the region under the recess and (ii) the degeneracy of the electron gas in the channel, which much reduces the emission of optical phonons (providing electron mobility in excess of $15\,000$ cm²/V s) so that the electrons injected into the drain region are nearly ballistic. Even if some of these effects could be overestimated in our simulations (i.e., higher mobilities and velocities than in the experimental devices), all of the conditions necessary for the onset of this ultrafast Gunn-like effect can be achieved in high mobility III-V heterolayers with submicrometer recess lengths. However, at present, a clear experimental confirmation of this effect is still lacking, which is not an easy task due to the very high frequencies involved.

IV. CONCLUSIONS

This paper proposes a new source of terahertz radiation obtained from a novel ultrafast Gunn-like effect happening in planar AlGaAs/InGaAs slot diodes. An ensemble MC simulation has been used to investigate the oscillations that emerge when the bias of the slot diode surpasses a threshold voltage given by the Γ - L intervalley energy. At this point, a kink appears in the I - V static characteristics and the instantaneous values of the current exhibit a coherent time-varying behavior at an extremely high frequency, leading to a pro-

nounced peak in its spectrum. It is demonstrated that terahertz frequencies are reached because of the presence of the ultrafast Γ electrons in the region of interest; this effect was achieved by means of the recess, which concentrates the voltage drop and injects very fast electrons into the drain region. Such ultrafast quasiballistic electrons appear mainly because of the degeneracy in the channel, which significantly reduces the rate of the scattering mechanisms and much increases the electron mobility. From the practical point of view, it is interesting that a simple frequency tuning of the terahertz radiation is possible by means of the applied voltage. These oscillations have also been found in the simulations of InAlAs/InGaAs HEMTs with the same layer structure in open channel conditions, a situation obtained for high gate-source voltages.

In order to exploit the full potential of these ultrafast Gunn-like diodes for the development of new terahertz MMICs, it would be interesting to study the dependence of the frequency and magnitude of the oscillations on different geometrical and technological parameters, as the lengths of the recess and recess-drain regions, δ doping, etc. This subject will be the objective of forthcoming works.

ACKNOWLEDGMENTS

This work was partially supported by Project No. TEC2007-61259/MIC from the Dirección General de Investigación (and FEDER) and Project No. SA044A05 from the

Consejería de Educación y Cultura de la Junta de Castilla y León.

- ¹*Terahertz Frequency Detection and Identification of Materials and Objects*, edited by R.E. Miles, X.-C. Zhang, H. Eisele, and A. Krotkus (Springer, New York, 2007).
- ²R. Köhler, A. Tredicucci, F. Beltram, H. E. Beere, E. H. Linfield, A. G. Davies, D. A. Ritchie, R. C. Iotti, and F. Rossi, *Nature (London)* **417**, 156 (2002).
- ³G. L. Carr, M. C. Martin, W. R. McKinney, K. Jordan, G. R. Neil, and G. P. Williams, *Nature (London)* **420**, 153 (2002).
- ⁴J. Łusakowski, W. Knap, N. Dyakonova, L. Varani, J. Mateos, T. Gonzalez, Y. Roelens, S. Bollaert, A. Cappy, and K. Karpierz, *J. Appl. Phys.* **97**, 064307 (2005).
- ⁵N. Dyakonova, A. El Fatimy, J. Łusakowski, W. Knap, M. I. Dyakonov, M. A. Poisson, E. Morvan, S. Bollaert, A. Shchepetov, Y. Roelens, Ch. Gaquiere, D. Theron, and A. Cappy, *Appl. Phys. Lett.* **88**, 141906 (2006).
- ⁶M. Dyakonov and M. Shur, *Phys. Rev. Lett.* **71**, 2465 (1993).
- ⁷J. Mateos, S. Pérez, D. Pardo, and T. González, IEEE Proceedings of the International Conference on Indium Phosphide and Related Materials, 2006 (unpublished), p. 313.
- ⁸S. Pérez, J. Mateos, D. Pardo, and T. González, *AIP Conf. Proc.* **922**, 197 (2007).
- ⁹G. M. Dunn, A. Phillips, and P. J. Topham, *Semicond. Sci. Technol.* **16**, 562 (2001).
- ¹⁰A. Khalid, N. J. Pilgrim, G. M. Dunn, M. C. Holland, C. R. Stanley, I. G. Thayne, and D. R. S. Cumming, *IEEE Trans. Electron Devices* **28**, 849 (2007).
- ¹¹J. Mateos, T. González, D. Pardo, V. Hoel, and A. Cappy, *IEEE Trans. Electron Devices* **47**, 250 (2000).
- ¹²J. Mateos, T. González, D. Pardo, V. Hoel, and A. Cappy, *IEEE Trans. Electron Devices* **47**, 1950 (2000).